Supporting Information for "Decadal predictability of the North Atlantic eddy-driven jet in winter"

Andrea Marcheggiani[1,2], Jon Robson[1], Paul-Arthur Monerie[1], Thomas J. Bracegirdle[3], and Doug Smith[4]

[1]National Centre for Atmospheric Science, Department of Meteorology, University of Reading, Reading, UK

[2]Geophysical Institute, University of Bergen, and Bjerknes Centre for Climate Research, Bergen, Norway

[3]British Antarctic Survey, Cambridge, UK

[4]Met Office, Exeter, UK

Contents of this file

1. Texts S1 to S3
2. Figures S1 to S2
3. Table S1

Introduction Supporting information included in this document comprises a list of the CMIP6 climate models contributing to the multi-model ensemble mean which all results are based on (Text S1 and Table S1), a more detailed discussion of NAO and eddy-driven

---

Corresponding authors: A. Marcheggiani (andrea.marcheggiani@reading.ac.uk), J. Robson (j.i.robson@reading.ac.uk)

jet mean states for each model individually (Text S2 and Figure S 1), and a brief overview of model skill at different lead times (Text S3 and Figure S 2).

Text S1 The multimodel ensemble is composed of the 10 different models that participated in the Component A of the DCPP (Boer et al., 2016). These are listed in Table S1.

Text S2

Figure S1 illustrates the mean states for the NAO and jet indices as a function of hindcast lead time for each of the models in Table S1. We notice that after year 3, most models have reached a stable state which does not necessarily fall within the observed variability (represented by the interquartile range from ERA5). Despite the large differences between the different models, the resulting skill of the multimodel ensemble mean is still significantly high (as shown in Fig. 2) and there is no significant relationship between a model's mean state and the corresponding skill.

Text S3

Figure S2 illustrates shows the skill scores (as measured by ACC) of the multimodel ensemble mean (non lagged) for different hindcast lead times. Panels at the top (Fig. S2a–c) show skill for the NAO, JLI and JSI over the *short* period, while panels below (Fig. S2d–f) refer to the *long* period. For the NAO and JSI, we observe high and statistically significant skill when we consider the earlier years in the hindcasts, especially over the *short* period (Fig. S2a,c). The skill at predicting the JLI (Fig. S2b) is visibly lower than that for the NAO and JSI, and does not appear to benefit from considering only the earlier year of the hindcast (low and statistically insignificant ACC in the bottom left corner of (Fig. S2b). In our study we consider the hindcast period 2–9. We exclude the first hindcast year (i.e. year lead start 1) as some DCPP-A model hindcasts are initialized at the end of December (BCC-CSM2-MR, CanESM5 and IPSL-CM6A-LR hindcasts), and thus do not provide a complete first winter season.

Table S1. List of climate models contributing to DCPP-A whose output is used in this study.

Institute	Model	Horizontal resolution	Ensemble size	Reference
Beijing Climate Center	BCC-CSM2-MR	100km	8	Xiao-Ge et al. (2019)
Canadian Centre for Climate Modelling and Analysis, Environment and Climate Change	CanESM5	500km	20	Swart et al. (2019)
National Center for Atmospheric Research	CESM1-1-CAM5-CMIP5	100km	40	Danabasoglu et al. (2020)
Centro Euro-Mediterraneo sui Cambiamenti Climatici	CMCC-CM2-SR5	100km	10	Cherchi et al. (2019)
Barcelona Supercomputing Center, Swedish Meteorological and Hydrological Institute	EC-Earth3	TL255	15	Döscher et al. (2021)
Met Office Hadley Centre	HadGEM3-GC31-MM	100km	10	Williams et al. (2018)
Institut Pierre-Simon Laplace	IPSL-CM6A-LR	250km	10	Boucher et al. (2020)
Center for Climate System Research, University of Tokyo, Japan Agency for Marine-Earth Science and Technology, National Institute for Environmental Studies	MIROC6	250km	10	Tatebe et al. (2019)
Max Planck Institute for Meteorology	MPI-ESM1-2-HR	100km	10	Müller et al. (2018)
Bjerknes Centre for Climate Research	NorCPM1	250km	20	Bethke et al. (2021)

References

Bethke, I., Wang, Y., Counillon, F., Keenlyside, N., Kimmritz, M., Fransner, F., ... others (2021). Norcpm1 and its contribution to cmip6 dcpp. *Geoscientific Model Development*, *14*(11), 7073–7116.

Boer, G. J., Smith, D. M., Cassou, C., Doblas-Reyes, F., Danabasoglu, G., Kirtman, B., ... others (2016). The decadal climate prediction project (dcpp) contribution to cmip6. *Geoscientific Model Development*, *9*(10), 3751–3777.

Boucher, O., Servonnat, J., Albright, A. L., Aumont, O., Balkanski, Y., Bastrikov, V., ... others (2020). Presentation and evaluation of the ipsl-cm6a-lr climate model. *Journal of Advances in Modeling Earth Systems*, *12*(7), e2019MS002010.

Cherchi, A., Fogli, P. G., Lovato, T., Peano, D., Iovino, D., Gualdi, S., ... others (2019). Global mean climate and main patterns of variability in the cmcc-cm2 coupled model. *Journal of Advances in Modeling Earth Systems*, *11*(1), 185–209.

Danabasoglu, G., Lamarque, J.-F., Bacmeister, J., Bailey, D., DuVivier, A., Edwards, J., ... others (2020). The community earth system model version 2 (cesm2). *Journal of Advances in Modeling Earth Systems*, *12*(2), e2019MS001916.

Döscher, R., Acosta, M., Alessandri, A., Anthoni, P., Arneth, A., Arsouze, T., ... others (2021). The ec-earth3 earth system model for the climate model intercomparison project 6. *Geoscientific Model Development Discussions*, 1–90.

Müller, W. A., Jungclaus, J. H., Mauritsen, T., Baehr, J., Bittner, M., Budich, R., ... others (2018). A higher-resolution version of the max planck institute earth system model (mpi-esm1. 2-hr). *Journal of Advances in Modeling Earth Systems*, *10*(7), 1383–1413.

Swart, N. C., Cole, J. N., Kharin, V. V., Lazare, M., Scinocca, J. F., Gillett, N. P., … others (2019). The canadian earth system model version 5 (canesm5. 0.3). *Geoscientific Model Development*, *12*(11), 4823–4873.

Tatebe, H., Ogura, T., Nitta, T., Komuro, Y., Ogochi, K., Takemura, T., … others (2019). Description and basic evaluation of simulated mean state, internal variability, and climate sensitivity in miroc6. *Geoscientific Model Development*, *12*(7), 2727–2765.

Williams, K., Copsey, D., Blockley, E., Bodas-Salcedo, A., Calvert, D., Comer, R., … others (2018). The met office global coupled model 3.0 and 3.1 (gc3.0 and gc3.1) configurations. *Journal of Advances in Modeling Earth Systems*, *10*(2), 357–380.

Xiao-Ge, X., Tong-Wen, W., Jie ZHANG, F. Z., Wei-Ping, L., Yan-Wu ZHANG, Y.-X. L., Yong-Jie, F., … others (2019). Introduction of bcc models and its participation in cmip6. *Advances in Climate Change Research*, *15*(5), 533.

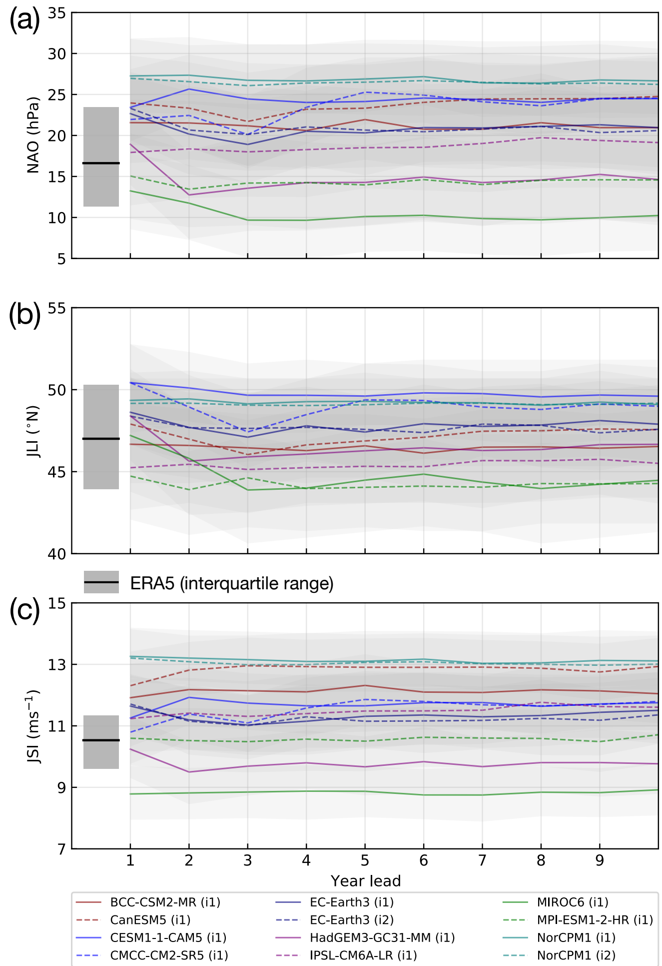

Figure S1. Evolution of the mean states of the NAO (a), Jet Latitude (b) and Jet Speed (c) indices as a function of lead year in the hindcasts for each of the CMIP6 DCPP models. Thick lines (solid and dashed) indicate the average of the index value across all ensemble members of each model contributing to the CMIP6 multi-model ensemble mean, while light shading represents the interquartile range associated with each model ensemble. On the left of each panel, the mean and interquartile range for ERA5 is shown (black line and dark gray shading) for ease of comparison.

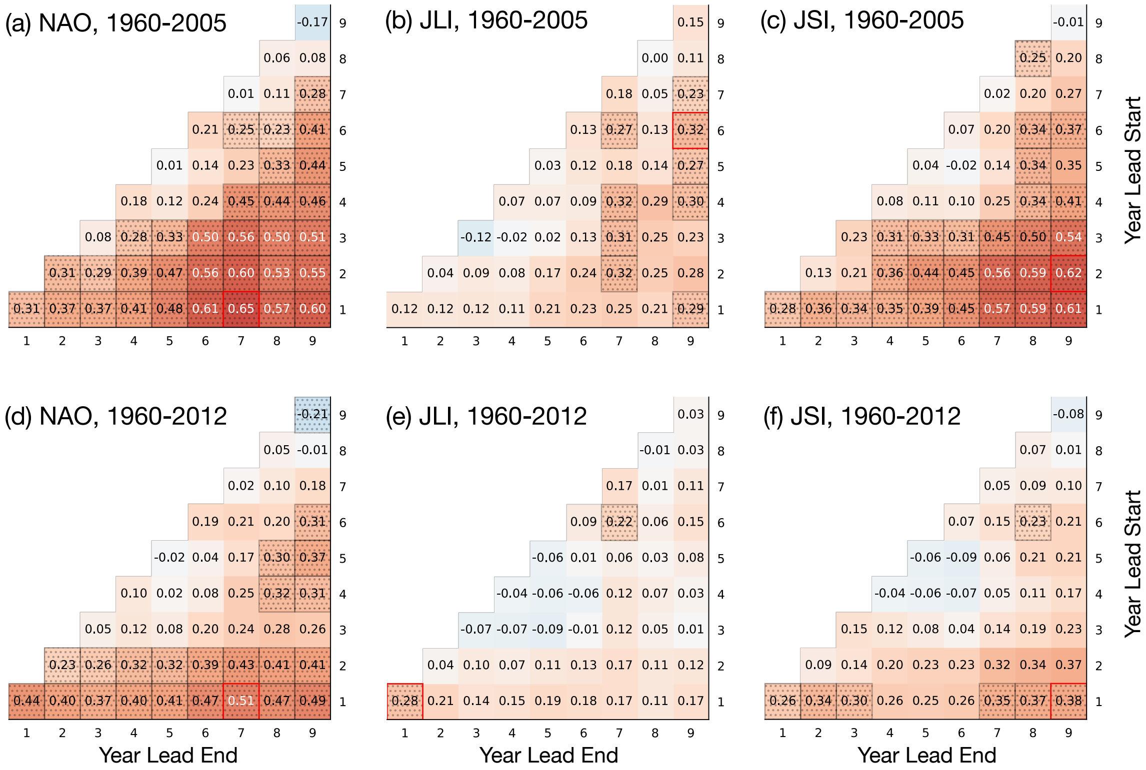

Figure S2. Skill scores as measured by ACC of the DCPP-A multimodel ensemble mean for different hindcast lead periods for the NAO (a,c), JLI (b,e) and JSI (c,f). Panels a–c refer to the *short* period, panels d–f to the *long* period. Each box indicates the ACC for the hindcast period starting from (and including) the year indicated on the right and ending on (and including) the indicated at the bottom of each panel. Color shading is proportional to the level of skill reported in each box (blue for negative, red for positive values), while statistical significance is indicated by hatching. The maximum level of skill is highlighted by red box edges.